Applied Catalysis A: General 504 (2015) 119–129

Contents lists available at ScienceDirect

Applied Catalysis A: General

journal homepage: www.elsevier.com/locate/apcata

# Improving the selectivity to C4 products in the aldol condensation of acetaldehyde in ethanol over faujasite zeolites

Lu Zhang[a], Tu N. Pham[a], Jimmy Faria[b], Daniel E. Resasco[a,*]

[a] School of Chemical, Biological, and Materials Engineering, University of Oklahoma, Norman, OK 73019, USA
[b] Abengoa Research, C/Energía Solar No. 1, Palmas Altas, Seville 41014, Spain

ARTICLE INFO

*Article history:*
Received 10 September 2014
Received in revised form
12 November 2014
Accepted 16 November 2014
Available online 22 November 2014

*Keywords:*
Aldol condensation
Acetaldehyde
Crotonaldehyde
Ethanol
Butadiene
Faujasite
Biomass.

ABSTRACT

The selective conversion of acetaldehyde to C4 products, minimizing the production of secondary (C6, C8) condensation products, could be a potential path in the production of butadiene from ethanol, a process of commercial interest. Therefore, we have investigated the selective aldol condensation of acetaldehyde in liquid phase over faujasite zeolites, NaX and NaY. Specifically, we have examined the influence of the number and location of the exchangeable cations, type of cations, and post-synthesis treatments on product selectivity. At 230 °C, NaY results in higher C4/(C6 + C8) product ratio than NaX, which can be explained in terms of the strength, density, and accessibility of basic sites, which are less favorable in NaX than NaY. In fact, the $CO_2$ TPD measurements indicate the presence of three types of basic sites of varying strength, of which those with weak and medium strength are most important for the selective condensation. A confinement effect is observed when adding K to the NaY zeolite. The observed selectivity changes suggest that when larger cations partially occupy the supercages, the production of C8 products decreases, while C6 products increase. Also, post-synthesis washing treatments show significant variations in selectivity, which demonstrate the effects of partial occupation of the zeolite pores in the reaction. It is also shown that at a given conversion, the C4/(C6 + C8) ratio can be adjusted by modifying the micro/mesoporosity balance in the zeolite.



## 1. Introduction

1,3-Butadiene (BD) is a building block in the chemical industry, used as a monomer or co-monomer in the production of polybutadiene, styrene–butadiene rubber and latex, acrylonitrile–butadiene–styrene resin, nitrile rubber, and styrene–butadiene block copolymers [1–3]. It is also used in the synthesis of monomer precursors, such as adiponitrile and chloropropene. The global demand for BD is on an annual scale of around 9 million tons [1]. Among the different approaches for the preparation of BD, steam cracking of paraffinic hydrocarbons accounts for over 91% of the world's butadiene supply. However, in this process, BD is a by-product of the manufacturing of ethylene [2]. Direct production of BD can be accomplished by catalytic dehydrogenation of *n*-butane and *n*-butene, as well as oxidative dehydrogenation of *n*-butene [1,3,4]. With increasing interest in utilizing renewable natural resources instead of fossil resources [5], it becomes important to investigate BD production routes from biomass. The abundant supply of ethanol from a variety of possible renewable sources makes it an attractive feedstock for the production of commodity chemicals, such as BD [6–13].

A possible strategy for the conversion of ethanol to BD includes the following steps: (i) dehydrogenation of ethanol to acetaldehyde; (ii) aldol condensation of acetaldehyde to crotonaldehyde; (iii) Meerwein–Pondorf–Verley (MPV) hydrogen transfer between ethanol and crotonaldeyde to produce crotyl alcohol; and (iv) dehydration of crotyl alcohol to BD [14–18]. Aldol condensation is a well-known reaction for C–C bond formation that can be catalyzed by either acid or basic catalysts [19–27]. Specifically, the aldol condensation of acetaldehyde has been investigated in several previous studies as an important intermediate reaction in the ethanol to BD process. In these studies [28–32], metal oxides, hydrotalcite, and amino acid have been used as catalysts, which exhibit varying extents of selectivity to C4 products. In this contribution, we have investigated the use of faujasite zeolites for the selective aldol condensation of acetaldehyde to C4 products, trying to minimize the excessive condensation to >C6 products.

Faujasite zeolites are commonly used in base-catalyzed reactions since the strength of their basic sites (framework O ions) can be adjusted by varying the Si/Al ratio and the electronegativity of

* Corresponding author.
*E-mail addresses:* resasco@ou.edu, ouresasco@gmail.com (D.E. Resasco).

http://dx.doi.org/10.1016/j.apcata.2014.11.018
0926-860X/

the exchangeable alkali metal cations used for compensating the negative framework charges [33–36]. At the same time, zeolites offer the possibility of controlling reaction selectivity by adjusting the extent of molecular confinement [37–39]. In consecutive reactions like the acetaldehyde self-condensation of interest in this work, the formation of the larger products (>C6) may be inhibited by confinement. This characteristic distinguishes zeolites from other types of basic catalysts and makes them a better candidate for obtaining high selectivities to C4 products since further condensation to heavier C6 and C8 hydrocarbons may be inhibited. While the aldol condensation of acetaldehyde in the vapor phase has been previously investigated on zeolite X [26], no reports have been found on the aldol condensation of acetaldehyde in liquid phase over faujasites, which is the focus of the present contribution. Moreover, in this work, we have investigated the aldol condensation in the presence of an alcohol, which can undergo hydrogen transfer via Meerwein–Pondorf–Verley (MPV) reaction and significantly affect the product distribution.

Specifically, in this study, we have examined NaX and NaY zeolites. While both zeolites have the FAU framework [40], the Si/Al atomic ratio for zeolite X is in the 1.0–1.5 range, while for zeolite Y is above 1.5 [41]. The effect of partially exchanging Na by K has been studied with zeolites KNaX and KNaY, with different post-synthesis washing procedures.

## 2. Experimental

### 2.1. Zeolite synthesis and treatment

The reagents used in the synthesis of all samples were purchased from Sigma-Aldrich and used as-received. They included sodium silicate (ca. 10.6% $Na_2O$ and 26.5% $SiO_2$), anhydrous sodium aluminate ($NaAlO_2$), sodium hydroxide (NaOH, ≥98%), potassium hydroxide (KOH, ≥85%), aluminate sulfate octadecahydrate, and potassium nitrate (≥99.0%).

The synthesis of zeolites NaX and NaY followed conventional methods reported in the literature. For zeolite NaX [42], a seed solution with a gel composition of 19 $Na_2O$:1.0 $Al_2O_3$:19 $SiO_2$:370 $H_2O$ was prepared by dissolving 2.1 g of NaOH in 12.36 g of distilled water; then, 0.51 g of $NaAlO_2$ and 13.44 g of sodium silicate were added to the mixture while stirring for 30 min in order to obtain a homogeneous clear solution. After standing at room temperature for 24 h, it was ready for use. To synthesize the zeolite, 2.05 g of $NaAlO_2$ was added to 20.98 g of distilled water and stirred for 10 min. Then, 1.68 g of NaOH, 8.49 g of sodium silicate, and 3.3 mL of the seed solution were added in sequence. The final solution was stirred at room temperature for 30 min before it was placed into Teflon bottles, where crystallization was allowed to occur at 100 °C for 4 h. The zeolite sample was obtained by separating the solid phase from the liquid phase and washed with distilled water until the pH of the mother liquid reached neutral. The resulting sample was calcined at 400 °C for 2 h and stored.

Zeolite NaY was synthesized by following the procedure described in US Patent No. 3,639,099. In this case, the seed solution was prepared to get a gel composition of 15.6 $Na_2O$:1.0 $Al_2O_3$:16 $SiO_2$:312 $H_2O$. For this, 2.1 g of NaOH were dissolved in 10.43 g of distilled water, and subsequently 0.51 g of $NaAlO_2$ and 11.32 g of sodium silicate were added. The mixture was stirred for 10 min until a homogeneous clear solution was obtained. It was allowed to stand at room temperature for 48 h before use in the next step. To synthesize the NaY zeolite, 1.67 g of aluminum sulfate, 28.30 g of sodium silicate, and 11.99 g of distilled water were mixed and stirred for 10 min. Then, 5 g of the as-prepared seed solution was added together with 1.64 g of $NaAlO_2$. The final solution was stirred at room temperature for 1 h. Once a homogeneous mixture was obtained, the solution was subdivided in smaller aliquots and placed into several Teflon bottles. Crystallization was carried out at 100 °C for 10 h. The zeolite sample was obtained by separating the solid phase from the liquid phase and washed with distilled water until the pH of the mother liquid was neutral. The washed solid was calcined at 400 °C for 2 h and stored.

The zeolite KNaX was synthesized by following the method reported by Kühl [43]. Specifically, the initial gel composition was 5.5 $Na_2O$:1.65 $K_2O$:1.0 $Al_2O_3$:2.2 $SiO_2$:122 $H_2O$. A typical procedure was as follows: 7.4 g of KOH, 11.67 g of NaOH, and 35.3 g of distilled water were mixed and subjected to vigorous stirring for around 5 min. At the same time, 6.56 g of $NaAlO_2$ and 20 g of distilled water were mixed and added to the former solution. Then, a mixture containing 19.9 g of sodium silicate and 20 g of water was added. The resultant solution was stirred at room temperature for 10 min and then transferred to Teflon bottles, which were capped and sealed with paraffin films. Crystallization was carried out first at 70 °C for 3 h and then at 100 °C for 2 h. Upon completion of the crystallization, the product was filtered and washed with distilled water. The as-synthesized sample was calcined at 400 °C for 2 h before the catalytic test.

The zeolite KNaY was obtained by ion-exchange on a pre-synthesized NaY, using 50 mL of the $KNO_3$ solution per g of NaY zeolite, based on a K/Na molar ratio of 2. After stirring for 6 h at room temperature, the exchanged zeolite was recovered by filtration and thoroughly washed with distilled water. In this case, as with all the other samples, the zeolite was calcined at 400 °C for 2 h before use.

### 2.2. Zeolite characterization

Powder diffraction (XRD) patterns were recorded in reflection geometry on a D8 Series II X-ray diffractometer (BRUKER AXS) that uses Cu Kα radiation generated at 40 kV and 35 mA. The elemental compositions of all zeolite samples were determined by ICP at Galbraith Laboratories. $N_2$ physisorption was performed on all samples by a Micromeritics ASAP 2010 unit. Prior to analysis, the zeolite samples were degassed in situ at 230 °C for 24 h. The micropore volume was derived from the *t*-plot method (relative pressure range: 0.2 – 0.6) and the total pore volume was determined at $p/p_0 = 0.99$. The mesopore size distribution was obtained by applying the BJH method to the data of the adsorption branch of the isotherm.

$^{27}Al$ NMR experiments were performed at Florida State University on a Bruker AVIII HD NMR spectrometer operating at a magnetic field strength of 11.74 T, equipped with a 4 mm Bruker MAS probe. For the MAS experiments of $^{27}Al$ (130.3754 MHz), a single pulse acquisition was applied with a spinning speed of 14 kHz, and a short RF pulse (less than 15°) with a recycle delay of 0.5–1 s. Spectra were collected after 10,240 scans and referenced to $AlCl_3$ (aq. 1 M) at 0 ppm.

The basicity of the catalysts was quantified by temperature-programmed desorption (TPD) of adsorbed $CO_2$ [44]. Before chemisorption, a 200-mg sample was heated in situ under a He flow of 30 mL/min with a heating rate of 10 °C/min up to 200 °C, holding at this temperature for 3 h. After cooling the sample to room temperature, it was exposed to a 30 mL/min flow of $CO_2$ for 30 min and then it was purged with He for 2 h to remove the physisorbed $CO_2$. The TPD was performed under the same He flow rate by heating from 0 to 600 °C with a heating rate of 10 °C/min.

### 2.3. Catalytic reaction measurements

The faujasite-catalyzed aldol condensation of acetaldehyde was carried out in the liquid-phase using a high-pressure 50-mL stainless steel autoclave batch reactor (Parr Corporation) equipped with impeller, temperature and pressure controllers, and sampling port. Ethanol was selected as the solvent to simulate conditions that

**Table 1**
Molar ratios (from ICP chemical analysis) and porosity characteristics of the zeolite samples.

| Catalyst | Si/Al | (K + Na)/Al | K/Na | $V_{micro}$ ($cm^3/g$) | $V_{meso}$ ($cm^3/g$) | $V_{meso}/V_{micro}$ |
|---|---|---|---|---|---|---|
| NaX | 1.28 | 0.99 | 0 | 0.267 | 0.144 | 0.539 |
| NaY | 2.14 | 1.03 | 0 | 0.362 | 0.039 | 0.108 |
| KNaX | 1.03 | 0.99 | 0.20 | 0.288 | 0.049 | 0.170 |
| KNaY | 2.08 | 0.92 | 2.65 | NA | NA | NA |
| KNaX (lower water) | 1.01 | 1.13 | 0.23 | 0.248 | 0.037 | 0.149 |
| NaX (lower water) | 1.25 | 1.07 | 0 | 0.225 | 0.085 | 0.378 |
| NaY (lower water) | 2.11 | 1.08 | 0 | 0.331 | 0.027 | 0.082 |
| NaOH-NaY | 2.10 | 0.99 | 0 | 0.324 | 0.047 | 0.145 |

might be encountered in the ethanol-to-BD process. In such a process, only a fraction of ethanol is dehydrogenated to acetaldehyde, which undergoes the aldol condensation; the unconverted ethanol can be used as a hydrogen source in the MPV reaction that converts crotonaldehyde to crotyl alcohol. Reaction temperature range was 130–230 °C, while the total pressure was kept at 300 psi. In a typical experiment, a measured amount of catalyst was mixed with acetaldehyde and ethanol in the reactor vessel. After the reactor was sealed, it was purged with $N_2$ to 300 psi, and heated up to the desired reaction temperature while stirring at 300−400 rpm. In all runs, the initial ethanol:acetaldehyde volume ratio was kept at 10:1 (2 mL of acetaldehyde). After a given period of time (6 or 12 h), the reaction was quenched by rapid cooling. Liquid products were filtered and analyzed using gas chromatography, GC–MS for product identification and GC–FID for quantification. Chemical standards were used to obtain the retention times and response factors for all reactants and products.

Determining the acetaldehyde conversion carries a large error because it is highly volatile at room temperature and during reaction can be formed from ethanol via dehydrogenation or MPV reaction. Therefore, the evaluation of the catalytic activity and selectivity of the different zeolite catalysts in the batch was made on the basis of the total moles of carbon in the products obtained during the given time period. At the beginning of the reaction, there are 72 mmol of carbon from 2 mL of acetaldehyde. However, since ethanol could partially convert into acetaldehyde, the carbon yield could in principle exceed 72 mmol. The selectivity is defined as the moles of carbon of a specific product to the total moles of carbon produced. The definitions are as follows:

$$C\ yield\,(mmol) = moles\ of\ carbon\ produced$$

$$C_4\ selectivity\,(\%) = \frac{moles\ of\ C4\ product \times 4}{Total\ moles\ of\ C\ in\ products} \times 100$$

$$C_6\ selectivity\,(\%) = \frac{moles\ of\ C6\ product \times 6}{Total\ moles\ of\ C\ in\ products} \times 100$$

$$C_8\ selectivity\,(\%) = \frac{moles\ of\ C8\ product \times 8}{Total\ moles\ of\ C\ in\ products} \times 100$$

## 3. Results and discussion

### 3.1. Characterization of zeolites NaX and NaY

XRD patterns were obtained to examine the crystallinity of the NaX and NaY zeolites (Fig. S1A). Each of the observed diffraction peaks for the two synthesized samples can be assigned to *hkl* reflections of FAU-type zeolites [45], without any additional peaks, which indicates that the two samples are pure faujasite zeolites. As expected, the calculated *d*-spacing for the NaY sample is smaller than the one for NaX, due to the higher Si/Al ratio in NaY than in NaX (see Table 1 for more information). This agrees with the relationship between the Si/Al ratio and unit cell sizes reported previously [46].

Fig. S1B shows the $^{27}Al$ MAS NMR spectra of zeolites NaX and NaY. A single peak is seen for both samples, with a chemical shift in the range of 55–68 ppm, which corresponds to the characteristic tetrahedral $Al(OSi)_4$ site of a perfectly crystalline faujasite [47] and is consistent with previously reported spectra [48]. No peak associated to octahedral extra-framework Al was found in the spectra, demonstrating the high crystallinity of the two catalysts. The slight difference in the chemical shift of the $^{27}Al$ signal in NaX (61 ppm) and NaY (59 ppm) may be ascribed to the different mean Al–O–Si bond angle in the framework [47].

The $N_2$ adsorption–desorption isotherms are included in Fig. S2. While zeolite NaY exhibited the characteristic isotherm of microporous materials [49], zeolite NaX displayed a clear hysteresis, indicating the presence of some mesoporosity and a lower microporosity than NaY. The use of NaOH during synthesis of NaX may cause partial desilication, which would account for the observed mesoporosity. All porosity values are summarized in Table 1, along with the elemental analysis of the zeolites investigated.

The TPD of adsorbed $CO_2$ provided a semi-quantitative evaluation of the strength and number of basic sites. Fig. 1 shows that, on NaX, the desorption of $CO_2$ started at about 50 °C, reached a maximum at about 100 °C, and was essentially completed at about 250 °C. Very small amounts desorbed at higher temperatures, showing broad peaks in the regions 300–350 and 400–450 °C. An approximate deconvolution of the profile (Fig. S3A) suggests the presence of four desorption peaks, centered at about 100, 150, 325, and 450 °C. Previous studies have assigned the different TPD-$CO_2$ peaks to different surface carbonate species, formed via the interaction of $CO_2$ with basic sites of varying strength [50–54]. Based

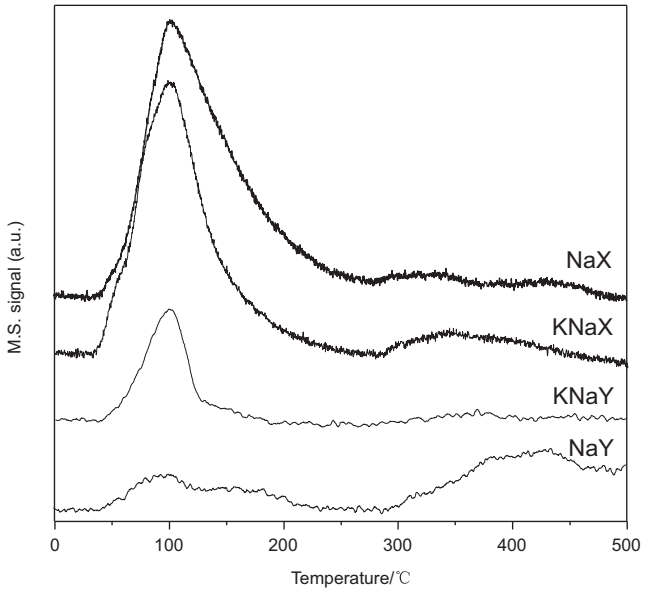


**Fig. 1.** TPD profiles of $CO_2$ over zeolite NaX, NaY, KNaX, and KNaY.

on these previous studies, the first two peaks could be ascribed to bicarbonate and bidentate carbonates species on basic sites of weak to medium strength. The two peaks at higher temperatures can be ascribed to unidentate carbonates on strong basic sites (see Scheme S1 in Supplementary Material for an illustration of the different carbonate species).

In marked contrast, the $CO_2$ TPD profile for NaY (Fig. 1) shows that not only the total desorbed amount was four-fold lower, but also the distribution of basicity strengths was very different. Assuming that adsorption of $CO_2$ was in a 1:1 stoichiometry [53], a comparison of total basic sites in NaX and NaY is presented in Table 2, which includes the TPD results for all the zeolites investigated. It is observed that the density of total basic sites is approximately four times higher in NaX than in NaY, which correlates with the lower Si/Al ratio of NaX and therefore its higher density of basic cations (Table 1). However, the most interesting observation is that the greatest difference is observed in the density of weak basic sites, that is, desorption below 250 °C. By contrast, the density of strong basic sites desorbing above 250 °C is not significantly different between the two catalysts.

**Table 2**
Density of basic sites of the zeolite samples as determined from $CO_2$ chemisorption.

| Catalyst | Total basic sites (μmol $CO_2$/g) | Number of basic sites for different peaks (μmol $CO_2$/g) | |
|---|---|---|---|
| | | Desorbed below $T$ = 250 °C | Desorbed above $T$ = 250 °C |
| NaX | 253.9 | 186.6 | 67.3 |
| NaY | 59.2 | 17.0 | 42.2 |
| KNaX | 224.7 | 192.3 | 32.4 |
| KNaY | 35.7 | 30.4 | 5.3 |
| KNaX (lower water) | 93.2 | 87.9 | 4.3 |
| NaX (lower water) | 236.8 | 193.7 | 43.1 |
| NaY (lower water) | 56.4 | 29.9 | 26.5 |

### 3.2. Catalytic activity of zeolites NaX and NaY

As shown in Scheme 1, self-aldol condensation of acetaldehyde produces 3-hydroxybutanal, which typically dehydrates readily to form crotonaldehyde. Another self-condensation pathway

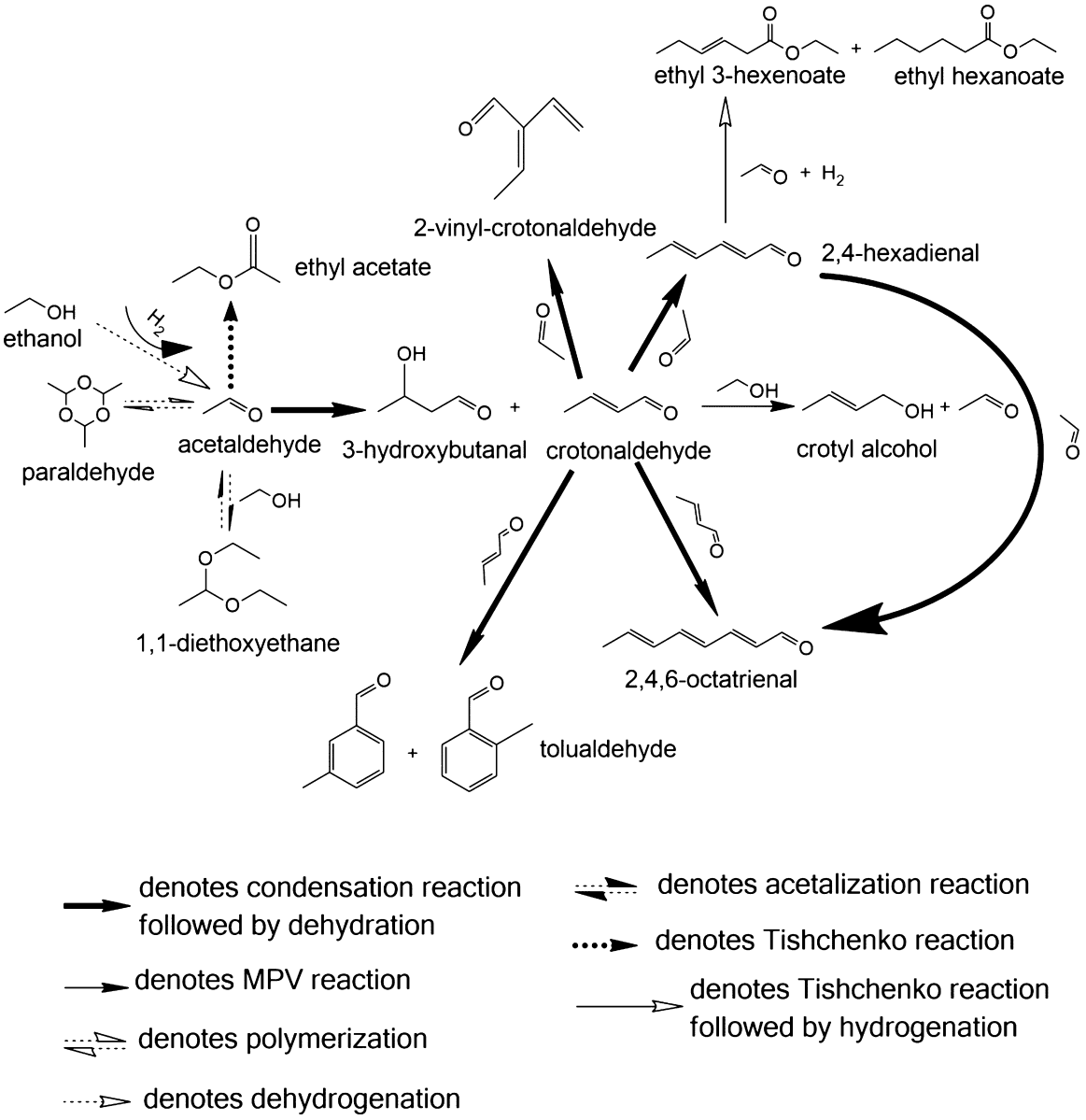


**Scheme 1.** Reaction network for acetaldehyde conversion over zeolite faujasite in liquid phase.

catalyzed by basic sites is the Tishchenko reaction [55] produces ethyl acetate. In addition, acetaldehyde can also oligomerize forming the trimer paraldehyde [56]. As shown in the scheme, 1,1-diethoxyethane is another possible product from the acid-catalyzed acetalization [57], in which one acetaldehyde molecule combines with two of ethanol. Fortunately, these two reactions are reversible and only important at low conversions. At longer reaction times, these products reverse to acetaldehyde, which undergoes aldol condensation reaction that becomes dominant. Therefore, these reactions do not inhibit the high selectivity to the desired C4 products.

However, crotonaldehyde can self-condense to C8 products (2,4,6-octatrienal and *meta*- or *ortho*-tolualdehyde) or can react with acetaldehyde to form C6 products (2,4-hexadienal and 2-vinyl-crotonaldehyde). 2,4-Hexadienal reacts with acetaldehyde to form 2,4,6-octatrienal (C8 product, by aldol condensation) or form ethyl 3-hexenoate and ethyl hexanoate (C8 products, by Tishchenko).

Finally, another crucial reaction in determining the overall selectivity is the MPV reaction, which is catalyzed by Lewis acids or bases. In the presence of ethanol, crotonaldehyde is reduced to form crotyl alcohol, while ethanol is oxidized to form acetaldehyde [58].

The activity and selectivity of the zeolites NaX and NaY for the aldol condensation of acetaldehyde in ethanol were evaluated in the batch reactor. As mentioned above, ethanol undergoes dehydrogenation and H transfer producing acetaldehyde [59]. Therefore, the catalytic performance was evaluated in terms of the amount of products obtained as a function of time. In the first set of experiments, the reaction was carried out at 130 °C for 12 h (Table 3). At this relatively low temperature, the carbon product yield from NaY was significantly higher than from NaX. However, over NaY only 1,1-diethoxyethane was produced, but no condensation products were obtained with this catalyst. By contrast, a small crotonaldehyde yield, but clearly higher than on NaY was observed over NaX, which is in line with the higher density of basic sites in NaX. While the selectivity to the undesired acetalization product (1,1-diethoxyethane) is very high on both catalysts at 130 °C, this reaction is reversible and, as seen in Table 3, the selectivity to this product greatly decreases as the reaction temperature increases. For instance, at 180 °C, the selectivity to condensation products (crotonaldehyde and 3-hydroxybutanal) after 12 h reaction over NaX increased to 27%. While the major product was still 1,1-diethoxyethane (about 66%) a clear trend was observed. Therefore, to further enhance the selectivity to condensation products, the reaction temperature was increased to 230 °C. To eliminate the catalyst deactivation issues for the comparison, reactions were performed over zeolite NaY for different reaction times. Since the acid-catalyzed acetalization is a reversible reaction and the product 1,1-diethoxyethane is converted back to the reactant (ethanol and acetaldehyde), only condensation product yields are compared here. As shown in Fig. S4 (Supplementary Materials), the condensation product yield increased almost linearly from 0, to 3 h, to 6 h. Moreover, it is observed that the C4/(C6 + C8) ratio is essentially unchanged (at about 5) for the first 6 h. The results indicate that there is no deactivation during the first 6 h (that is total condensation yield after 6 h is twice as that of 3 h). Based on the results, 6 h of reaction time was chosen for the comparison discussed below.

**Table 3**
Catalytic performance of zeolites NaX and NaY (mass 400 mg) for aldol condensation of acetaldehyde.

| Catalyst | NaX | | | NaY | | |
|---|---|---|---|---|---|---|
| Reaction temperature (°C) | 130 | 180 | 230 | 130 | 180 | 230 |
| Reaction time (h) | 12 | 12 | 6 | 12 | 12 | 6 |
| Product C yield (mmol) | 24.8 | 25.8 | 29.0 | 42.2 | 21.3 | 33.2 |
| *Carbon selectivity* (%) | | | | | | |
| 1,1-Diethoxyethane | 94.2 | 65.7 | 10.7 | 100.0 | 74.4 | 15.7 |
| Crotonaldehyde | 5.8 | 23.5 | 48.7 | 0.0 | 18.7 | 51.3 |
| 3-Hydroxybutanal | 0.0 | 3.5 | 4.6 | 0.0 | 2.5 | 4.4 |
| Crotyl alcohol | 0.0 | 0.0 | 4.1 | 0.0 | 0.0 | 4.8 |
| Ethyl acetate | 0.0 | 6.1 | 11.2 | 0.0 | 4.4 | 8.6 |
| Paraldehyde | 0.0 | 0.0 | 0.0 | 0.0 | 0.0 | 3.3 |
| Mixed condensation C6 | 0.0 | 0.0 | 3.2 | 0.0 | 0.0 | 1.8 |
| Mixed condensation C8 | 0.0 | 1.2 | 17.5 | 0.0 | 0.0 | 10.0 |

Reported as overall product C yield and product distribution. Batch reactor at varying temperatures, $N_2$ pressure 300 psi, stirring rate 300–400 rpm, solvent (ethanol)/reactant (acetaldehyde) volume ratio 10 with acetaldehyde 2 mL.

Table 3 shows that similar carbon product yields were obtained over the two catalysts, that is, 29.0 mmol on NaX and 33.2 mmol on NaY. The decrease in acetalization selectivity was sharper on NaX, but the selectivity to C4 products (crotonaldehyde, 3-hydroxybutanal, and crotyl alcohol) greatly increased on both catalysts. Accompanying the increase in desirable products, heavier condensation products such as C6 and C8 began to appear in significant yields on both catalysts. However, NaY seemed to exhibit a much lower selectivity to C6–C8 products than NaX at comparable C4 yields.

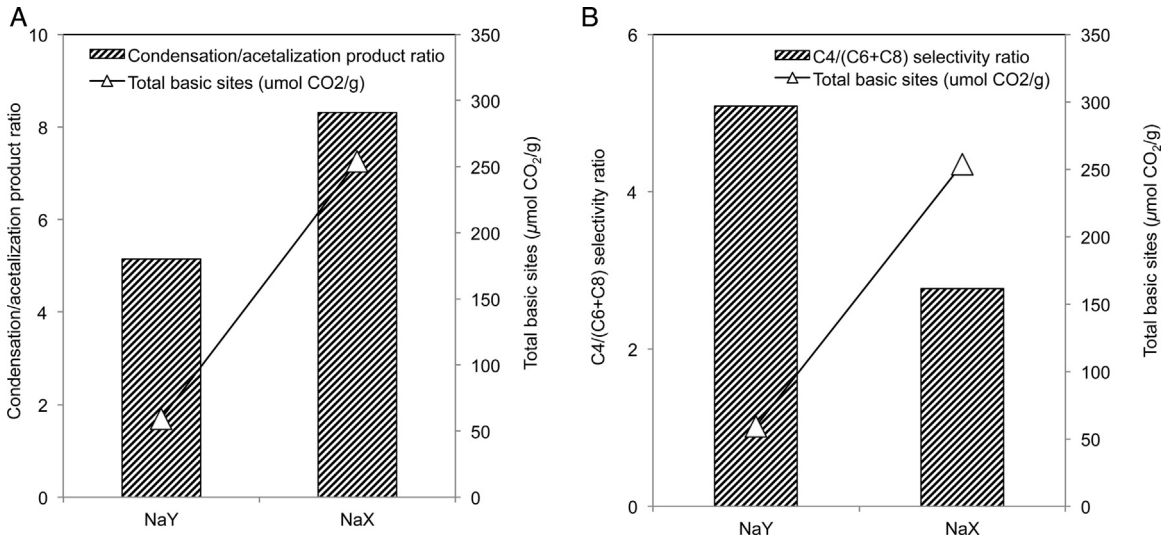


**Fig. 2.** Product distribution from acetaldehyde conversion at 230 °C and 300 psi and basicity of zeolites NaX and NaY.

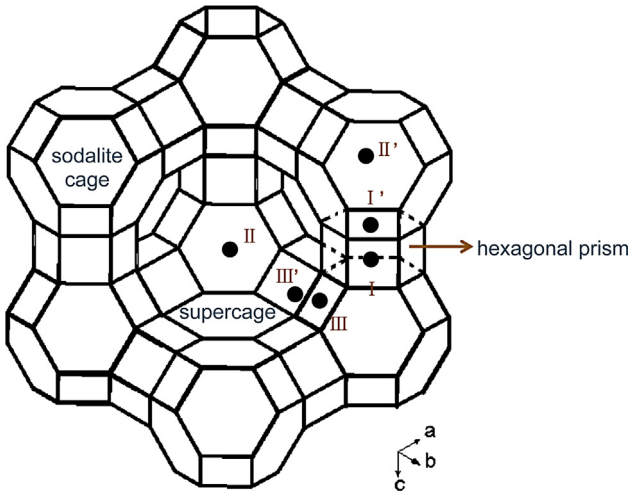


**Fig. 3.** Location of cations in zeolites NaX and NaY.

A comparison between desirable and undesirable products on the two zeolites is made in Fig. 2. Clearly, with a higher density of basic sites, NaX exhibits a higher condensation/acetalization product molar ratio than NaY (Fig. 2A). However, excess density of basic sites may be adverse to maximize C4 condensation products (crotonaldehyde, 3-hydroxybutanal, and crotyl alcohol). As seen in Fig. 2B, with essentially the same overall yield, the C4/(C6 + C8) ratio is nearly twice on the less basic NaY than on the more highly basic NaX.

The location and proximity of basic sites in the faujasite zeolites may significantly vary from NaX to NaY. It is well known that $Na^+$ ions may occupy different in the faujasite structure, as illustrated in Fig. 3 [60–62]. One can see that the so-called site I is in the hexagonal prism, while site I′ is in the sodalite cage, facing the position of site I. Similarly, site II is at the center of the hexagonal window inside the supercage, while site II′ is in the sodalite cage, facing position II. Finally, site III is located above a square window between two other square windows and site III′ is at the edge of the square window.

The location of $Na^+$ cations at sites I, I′, II, and III′ in NaX were demonstrated by Olson [63], using single-crystal X-ray diffraction. By contrast, in zeolite NaY, the $Na^+$ cations only occupy sites I, I′, and II. It is well known that the basicity of a zeolite can be ascribed to negatively charged framework O atoms close to the cations [51]. That is, lower Si/Al ratios require more exchangeable cations and therefore results in higher basicity. In this case, NaX has a larger number of cations than NaY and consequently a higher density of basic framework O atoms, connected to the cations located at the specific sites described above [64]. Therefore, these basic sites are located inside and outside the supercages.

One can explain the observed differences in C4/(C6 + C8) ratios in terms of the density and location of the basic sites. A larger number of exchangeable cations occupy the supercage in NaX than in NaY. This could result in possible confinement effects. Pidko and van Santen [65] have emphasized that in low-silica zeolites, where the density of exchangeable cations is high, the intrazeolite arrangement of cations plays a crucial role in activity and selectivity since these ions can undergo multiple noncovalent interactions with the reactants, resembling the active sites encountered in enzymes. Such interactions are present even with small molecules such as $N_2O_4$ [66].

We should expect a larger concentration of cations inside the supercages in NaX, which may hinder the base-catalyzed condensation, but also acetalization, which is catalyzed by Lewis acid sites inside the cages. Thus, only the basic sites outside the supercages, active for condensation are left available. These sites, without much steric constrains, may favor both condensation to C4 and overcondensation to C6 and C8 products.

By contrast, NaY has a lower density of basic sites either inside or outside the supercage, but, the accessibility to the internal cavities is higher in this zeolite than in NaX; thus, when acetaldehyde is converted into C4 inside the zeolite, the possibility of further condensation to larger products such as C6 or C8 is more inhibited than in the case of NaX. This confinement effect should result in a higher selectivity to the C4 product that can leave the zeolite without further reaction. At the same time, the lower density of basic sites outside the cage further decreases the rate of over-condensation of C4 products outside the supercages. We should also point out that the lower density of basic sites in NaY fails to prevent the acid-catalyzed acetalization, which is greatly reduced in NaX (Fig. 2A).

### 3.3. *Catalytic activity of zeolites NaX and NaY after pre-adsorption of $CO_2$*

Another important point to interpret the changes in selectivity among different faujasite zeolites is the role played by the different distribution of basicity strengths of the sites in NaX and NaY. The following experiment was conducted to determine whether only the stronger basic sites (i.e., those responsible for $CO_2$ desorption above 300 °C) are active for acetaldehyde condensation. The NaX or NaY catalyst was first exposed to $CO_2$ and then tested under the same 230 °C conditions. At 230 °C, the $CO_2$ adsorbed on the weak basic sites would have left the surface but that one adsorbed on the strong basic sites should still remain on the surface blocking those sites.

For NaX, the majority of the $CO_2$ desorption occurs below 250 °C (Fig. 1). Then, with the reaction temperature of 230 °C, only a small fraction of basic sites is blocked by $CO_2$. Table 4 shows the total carbon product yields and the selectivities to products over the

**Table 4**
Catalytic performance of zeolites NaX, NaY, KNaX, and KNaY for aldol condensation of acetaldehyde.

| Catalyst | NaX | NaX ($CO_2$) | KNaX | NaY | NaY ($CO_2$) | KNaY |
|---|---|---|---|---|---|---|
| Product C yield (mmol) | 29.0 | 22.4 | 32.8 | 33.2 | 29.4 | 24.0 |
| *Carbon selectivity (%)* | | | | | | |
| 1,1-Diethoxyethane | 10.7 | 12.2 | 9.3 | 15.7 | 29.4 | 27.1 |
| Crotonaldehyde | 48.7 | 46.6 | 42.1 | 51.3 | 39.9 | 40.6 |
| 3-Hydroxybutanal | 4.6 | 4.5 | 4.2 | 4.4 | 3.7 | 3.1 |
| Crotyl alcohol | 4.1 | 3.9 | 3.8 | 4.8 | 1.6 | 3.0 |
| Ethyl acetate | 11.2 | 12.7 | 9.8 | 8.6 | 11.7 | 14.3 |
| Paraldehyde | 0.0 | 0.0 | 0.0 | 3.3 | 4.7 | 3.1 |
| Mixed condensation C6 | 3.2 | 3.4 | 2.6 | 1.8 | 1.9 | 7.0 |
| Mixed condensation C8 | 17.5 0.1 | 16.8 0.1 | 28.2 0.2 | 10.0 0.5 | 7.2 1.1 | 1.9 0.5 |
| Condensation product yield/number of basic sites C4/(C6 + C8) | 2.8 | 2.7 | 1.6 | 5.1 | 5.0 | 5.2 |

Reported as overall product C yield and product distribution. Batch reactor at 230 °C, reaction time 6 h, catalyst mass 400 mg, $N_2$ pressure 300 psi, stirring rate 300–400 rpm, solvent (ethanol)/reactant (acetaldehyde) volume ratio 10 with acetaldehyde 2 mL with or without exposure to $CO_2$, as an inhibitor of basic sites.

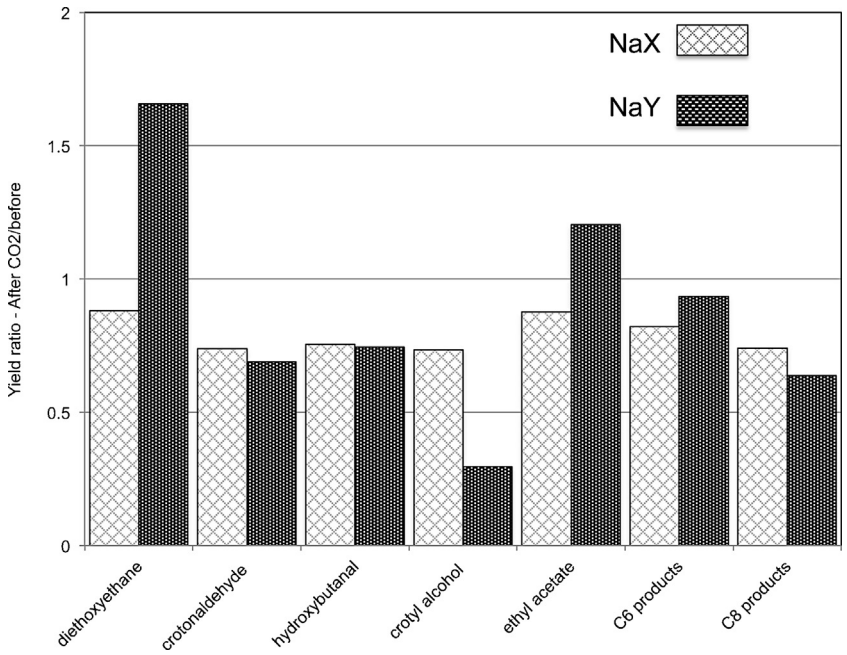


**Fig. 4.** Variation of product yield after exposure of zeolites NaX and NaY to $CO_2$ as an inhibitor of basic sites expressed as the ratio of individual product yields obtained with and without exposure to $CO_2$. Reaction temperature 230 °C, reaction time 6 h, catalyst weight 400 mg, solvent (ethanol)/reactant (acetaldehyde) volume ratio 10, acetaldehyde 2 mL.

$CO_2$-loaded zeolites. For NaX, only a slight decrease in total product yield (22.4 mmol vs. 29.0 mmol) was observed. This result indicates that only a small fraction of the activity can be ascribed to the strong basic sites. As shown in Fig. 4, a small loss in yield was observed for all products after exposure to $CO_2$, with a moderately higher loss in yield for the condensation C4, C6, and C8 products than for those catalyzed by acid sites. For NaY, the situation is somewhat different. While the overall loss in total product yield was relatively small after exposure to $CO_2$ (i.e., 29.4 from 32.2 mmol), the change in product distribution was much more pronounced than that on NaX. As seen in Fig. 4, the yield of acid-catalyzed reaction products increased significantly, but the condensation C4, C6, and C8 products greatly decreased, which is consistent with the $CO_2$ TPD measurements that show that a large fraction of sites was able to hold $CO_2$ up to temperatures significantly higher than the reaction temperature.

Fig. 5A compares the condensation/acetalization product ratios before and after $CO_2$ loading on each catalyst. The ratio only decreased by less than 15% over $CO_2$-loaded NaX, but by about 50% over $CO_2$-loaded NaY. These results indicate that in NaY, with a small number of basic sites present and a significant fraction being covered by $CO_2$, the carbon yield remained high due to the acetalization reaction, which can be catalyzed by Lewis acid sites ($Na^+$ ions); the yield loss was specifically on the base-catalyzed condensation products.

Interestingly, as shown in Fig. 5B, the C4/(C6 + C8) ratio was practically unchanged for either catalyst after exposure to $CO_2$. This may suggest that all basic sites catalyze both the formation of C4 and its subsequent condensation, simultaneously.

### 3.4. Catalytic activity of zeolites KNaX and KNaY

As mentioned above, a high basic site density can only be accomplished at low Si/Al ratios, which require a large number of exchangeable cations. Low-silica zeolites with Si/Al ratios close to unity can be achieved with zeolites KNaX, which can result in the maximum possible number of cations per unit cell [67]. Therefore, to investigate the influence of the number of cations in the zeolite, a KNaX with low Si/Al ratio was synthesized and tested for the aldol condensation reaction. Similar to NaX, the cations in KNaX are stabilized at sites I, I′, II, and III′, with $K^+$ ions replacing part of the $Na^+$ ions at sites I′ [68,69]. The KNaX zeolite has more exchangeable cations per supercage and therefore one can expect a higher number of basic sites on the external surface than NaX [68,69].

The synthesized KNaX zeolite was thoroughly characterized by XRD, $^{27}Al$ NMR, atomic composition, and $N_2$ adsorption. The characterization results of the KNaX material are included in the Supplementary Material. They clearly indicate that the synthesized zeolite is a highly pure and crystalline FAU-type material (Supplementary Material, Fig. S5). It has a Si/Al ratio of around one and K/Na ratio of 0.2 (Table 1). The $N_2$ adsorption–desorption isotherms demonstrate its microporous characteristics and also the presence of small mesopore volume (Supplementary Material, Fig. S6).

The results from the $CO_2$ TPD (Table 2) would imply that KNaX has a slightly lower basic site density than NaX. However, this result must be analyzed with some detail, due to its lower Si/Al ratio, the zeolite KNaX has a larger number of exchangeable cations than NaX and, consequently, should have a higher density of O atoms with basic characteristics. However, the TPD results do not reflect this higher density. This discrepancy could be due to the higher density of cations in the supercages and sodalities cages, which may limit the number of $CO_2$ molecules that can be accommodated in these cavities. In addition, the $CO_2$ TPD profile of KNaX (Fig. 1) shows a clear difference in the shape of the low-temperature peak compared to that of NaX. The narrower peak of the former might indicate that some of the medium-strength basic sites present in the latter are eliminated. It is reasonable to ascribe this change to the larger ionic radius of $K^+$ compared to $Na^+$, which could result in weaker interactions with $CO_2$ [50].

The catalytic results of the acetaldehyde condensation over KNaX tested at 230 °C are presented in Table 4 and should be compared to those obtained on NaX under the same conditions. While both catalysts exhibited about the same total product yield, KNaX

gave a lower selectivity to the acetalization reaction but at the same time it favored C8 product over the C4 condensation products.

These selectivity differences can be interpreted in terms of the confinement effects mentioned above. That is, when the cation concentration inside the supercages is too high, not even the initial condensation of C2–C4 takes place inside these cavities. Clearly, with even less accessible space in the supercage and more basic sites on the external sites, condensation to C4 and over-condensation to C8 products occur at comparable rates, thus lowering the C4/(C6 + C8) ratio.

To examine the effect of incorporating $K^+$ ions into the NaY zeolite, a KNaY zeolite was prepared by ion-exchange. The resulting K/Na ratio determined by ICP was found to be about 2.7. The XRD pattern and $^{27}$Al NMR spectrum show the high crystallinity and structural integrity of KNaY, as compared to NaY (Supplementary Material, Fig. S7). The catalytic results of KNaY, obtained at 230 °C, under the same conditions as those used for the other zeolites are included in Table 4.

Compared to NaY, KNaY shows a lower carbon yield with a decrease of about 14% in the desirable C4 product selectivity and an increase of about 11% in selectivity to the less desirable 1,1-diethoxyethane. Furthermore, a significant change in the C6/C8 ratio was observed. While on NaY, C8 was much larger than C6, the opposite is true on KNaY. The $CO_2$ TPD plot indicates that KNaY contains less (accessible) basic sites than NaY (Table 2, see Fig. S8A in Supplementary Material for the deconvoluted TPD profile). As discussed in the case of KNaX, this decrease results from two factors: the incorporation of $K^+$ ions inside the cages of the zeolite, which are larger than $Na^+$ and may block the access of molecules, and the weaker interaction between the basic sites induced by $K^+$ and $CO_2$.

In contrast to NaY, which has low density of basic sites but the majority are strong, when K is incorporated, the KNaY shows a much lower density of strong basic sites. Again, the disappearance of the strong sites from NaY can be ascribed to the weaker polarizing strength of $K^+$ compared to $Na^+$ [50,70].

The observed changes in the C6/C8 ratio may be due to the increased confinement caused by the replacement of smaller $Na^+$ by larger $K^+$ ions, which leave less space available for condensation of two C4 molecules that form C8, compared to one C4 and one C2 that form C6 products. The increase in the acetalization reaction might result from some degree structural collapse that may occur during ion exchange [71]. With some cations in the sodalite cages exposed to acetaldehyde and ethanol, the Lewis acid-catalyzed acetalization may be accelerated.

### 3.5. Catalytic activity of zeolites NaX and NaY with different extent of post-synthesis washing

The synthesis of zeolites proceeds in a highly alkaline environment. After crystallization, zeolites are usually separated from the mother liquid and completely washed using large amounts of distilled water. For example, the zeolites NaX and NaY discussed above were washed until pH was close to neutral. For KNaX, it was washed until pH reached 9 to avoid hydrolysis [43]. If the zeolites are washed using lower amounts of water, occluded cations may remain in the zeolite and the properties and catalytic activity may vary significantly. We have examined the effect of different extents of post-washing on the activity and selectivity for acetaldehyde reaction. In this case, with zeolites NaX and NaY, post-washing was stopped when pH 9 was reached instead of 7, as in the standard case. Likewise, for the KNaX, the washing step was stopped at pH 11 instead of 9, as above. These zeolites, with lower extents of washing are identified here as NaX (lower-water), NaY (lower-water), and KNaX (lower-water).

**Table 5**
Catalytic performance of zeolites KNaX, NaX, and NaY using lower amount of water than the standard procedure.

| Catalyst | KNaX | NaX | NaY |
|---|---|---|---|
| Product C yield (mmol) | 31.8 | 27.2 | 29.4 |
| *Carbon selectivity* (%) | | | |
| 1,1-Diethoxyethane | 23.0 | 6.9 | 13.1 |
| Crotonaldehyde | 26.3 | 42.7 | 49.4 |
| 3-Hydroxybutanal | 3.5 | 5.0 | 5.2 |
| Crotyl alcohol | 3.5 | 3.5 | 3.6 |
| Ethyl acetate | 7.5 | 9.9 | 9.8 |
| Paraldehyde | 0.0 | 0.0 | 1.9 |
| Mixed condensation C6 | 4.0 | 2.5 | 3.8 |
| Mixed condensation C8 | 32.2 | 29.4 | 13.2 |

Reported as overall product C yield and product distribution. Batch reactor at 230 °C, reaction time 6 h, catalyst weight 400 mg, $N_2$ pressure 300 psi, stirring rate 300–400 rpm, solvent (ethanol)/reactant (acetaldehyde) volume ratio 10 with acetaldehyde 2 mL.

The XRD patterns did not differ from those with the more extensive washing. They had only the peaks expected for the corresponding faujasite. Similarly, the $^{27}$Al NMR spectra only displayed the signal of the tetrahedrally coordinated framework Al (Supplementary Material, Fig. S6), demonstrating that the degree of crystallinity remained high. As shown in Table 1, the elemental analysis shows that the Si/Al ratio of the zeolites washed with low amount of water kept the same Si/Al ratio as the corresponding clean ones. However, these zeolites (lower-water) resulted in an excess of alkali cations compared to Al; that is, the (K + Na)/Al ratio for KNaX (lower-water) was 1.13, compared to 1.03 for the clean KNaX. Further, as also shown in Table 1, the zeolites (lower-water) had smaller $V_{micro}$ and $V_{meso}$ than the corresponding clean zeolites. It is clear that the lower-water zeolites contained extra alkali cations that block some of the internal cavities of the zeolites. Consistently, the $CO_2$ TPD data indicate that these impurities block some of the pores, resulting in a lower density of accessible basic sites (Table 2, see Fig. S8B–D in Supplementary Material for the deconvoluted TPD profiles).

Table 5 shows the catalytic performances of the zeolites washed with lower amounts of water and thus containing excess alkali cations. The three types of zeolites (lower-water) gave similar carbon yields to the corresponding clean ones (Tables 3 and 4). However, the product selectivity showed a significant variation. A detailed comparison of the product distribution obtained over the lower-water and clean zeolites is made in Fig. 6. Clearly, over the lower-water zeolites, the condensation/acetalization product ratio was higher, but the C4/(C6 + C8) ratio was lower. That is, with the alkali impurities occluded in the zeolite cavities, the reactions tended to proceed outside the supercages. Therefore, these lower-water zeolites were less shape selective. Likewise, the condensation/acetalization product ratio was much lower over lower-water KNaX than over the clean KNaX (Fig. 6), which can be explained with the same arguments mentioned for the other zeolites. Interestingly, the same selectivity and yields as those obtained on the clean KNaX can be reproduced (Supplementary Material, Fig. S9) when the lower-water KNaX was rewashed in warm water (around 50 °C). These results demonstrate that the observed differences are simply due to the presence of occluded alkali cations, which can be easily removed by more extensive washing.

Fig. 6 compares the condensation/acetalization and the C4/(C6 + C8) ratios. Both are desirable product ratios in this study, but they vary in opposite directions. In principle, one would conclude that the overall basicity is the main effect responsible for this trend; that is, a higher basicity should result in higher condensation/acetalization ratio and lower C4/(C6 + C8). However, as shown

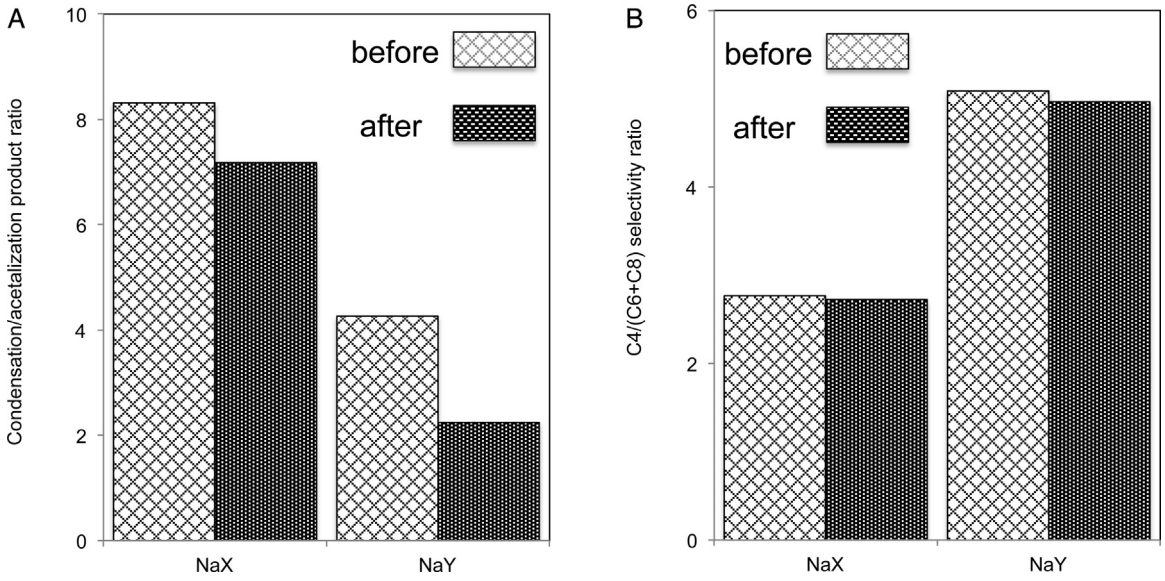


**Fig. 5.** Product ratios over NaX and NaY, before and after exposure to $CO_2$. (A) Condensation/acetalization ratio; (B) C4/(C6 + C8) condensation product ratio. The solvent (ethanol) to reactant (acetaldehyde) ratio was 10 by volume with acetaldehyde 2 mL. The reaction temperature was 230 °C and reaction time was 6 h. The catalyst weight was 400 mg.

in Table 4, the condensation yield does not increase with the density of basic sites. In fact, the apparent yield/site rates are much lower in NaX than NaY zeolites. The latter produces about the same amount of condensation products as the former, but with a much lower density of basic sites. At the same time, C4/(C6 + C8) is much higher on the NaY catalysts. These results are in good agreement with the concepts mentioned above regarding the effect of accessibility and confinement. That is, the supercages in NaY zeolites are more accessible than those of NaX and, particularly KNaX. In those cases, the acid sites responsible for acetalization are more available, lowering the condensation/acetalization ratio. At the same time, the greater accessibility plays a role in the C4/(C6 + C8) ratio, enhancing the production of C4 and reducing the over-condensation. By contrast, on NaX, KNaX, and even more on the lower-water zeolites, the majority of the cavities are not accessible for condensation reactions. Thus, they occur on the external basic sites, which cannot

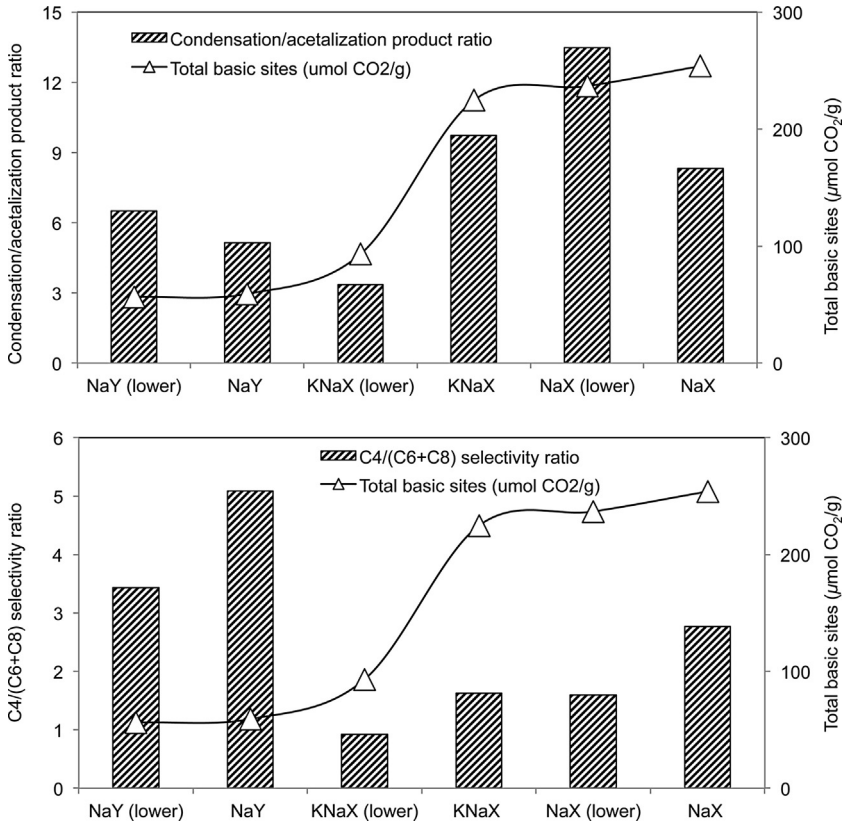


**Fig. 6.** Comparison among zeolites KNaX, NaX, NaY, and the corresponding not fully washed zeolites (lower-water). Reaction temperature 230 °C, reaction time 6 h, catalyst weight 400 mg, solvent (ethanol)/reactant (acetaldehyde) volume ratio 10, acetaldehyde 2 mL.

benefit by shape-selective effects, which lowers the C4/(C6 + C8) ratio.

To further evaluate the effect of confinement and mobility inside the zeolite, a NaY containing enhanced mesoporosity was prepared by dispersing 1 g of the NaY sample in 50 mL of 0.1 M NaOH solution. Upon stirring at room temperature for 30 min, the solid sample was obtained by filtration and completely washed using distilled water.

The immersion in NaOH results in partial desilication and generation of mesopores. In fact, the $N_2$ adsorption–desorption isotherms indicate that the $V_{meso}/V_{micro}$ ratio of the resulting NaOH-NaY sample is 0.145, which is about 34% higher than that of NaY. The mesopore size distribution graph (Supplementary Material, Fig. S10) shows that NaOH-NaY contains an additional peak at around 12 nm, which reveals the presence of some additional mesoporosity in the NaOH-NaY material. The catalytic comparison between NaY and NaOH-NaY tested under the 230 °C conditions is shown in the Supplementary Material (Fig. S11). Clearly, a lower condensation/acetalization product ratio and a higher C4/(C6 + C8) ratio were obtained over the NaOH-NaY catalyst, which supports the concept that reduced confinement and enhanced mobility inside the zeolite has a positive impact on the intermediate condensation toward C4 products, but at the same time sacrifices selectivity relative to the acid-catalyzed acetalization.

### 3.6. Role of ethanol as a solvent

To examine whether the ethanol solvent plays a direct role in the reaction, a blank experiment was performed using only ethanol as a feed while keeping the same catalyst (400 mg NaY) and reaction conditions unchanged (230 °C and 6 h). The result of the blank test shows that the ethanol conversion was about 5.4% and the products included acetaldehyde, 1,1-diethoxyethane, and small amounts of crotonaldehyde, which derive from the acetaldehyde produced. That is, the contribution of ethanol to the condensation reaction is minimal. However, ethanol as a solvent plays an important role in preserving the catalyst activity. In fact, when ethanol was replaced by *n*-hexane as the solvent, the initially white NaY catalyst became black after the reaction, a color change that was not observed when ethanol was the solvent and reflects the ability of ethanol to prevent coke formation by limiting the formation of heavy condensation products via the MPV H-transfer reaction described above.

## 4. Conclusions

A series of NaX and NaY zeolites have been compared as catalysts for the aldol condensation of acetaldehyde in the liquid phase, using ethanol as a solvent and co-reactant. The target desirable product is the first dimer condensation product (C4). However, at moderately low temperatures (130–180 °C), the dominant reaction is acetalization, producing 1,1-diethoxyethane. The preferred condensation C4 products, including crotonaldehyde, 3-hydroxybutanal, and crotyl alcohol only become major products at about 230 °C, but the C4/(C6 + C8) selectivity is a strong function of the type of catalyst investigated.

It was found that, when compared at similar carbon product yields, the NaX results in higher condensation/acetalization ratio but lower C4/(C6 + C8) ratio than NaY. These differences can be ascribed not only to the higher basicity of NaX, but also to the larger number of exchangeable cations per supercage. With a more highly occupied cage and higher density of basic sites on the external surface, NaX has higher activity for the condensation reactions but lower selectivity to the desirable C4 products. By contrast, on the NaY zeolite, the acid-catalyzed acetalization lowers the condensation/acetalization ratio, but enhances the C4/(C6 + C8) ratio due to a more effective shape selectivity. This conclusion is further supported by the comparison between KNaY and NaY. The enhanced shape selectivity of NaY becomes more significant upon introducing $K^+$ ions in the supercage, as reflected by the more pronounced decrease in C8 condensation product compared to C6.

Plugging sites inside the supercages while leaving external sites accessible by either increasing the number of alkali cations or reducing the extent of post-washing treatment all have the same general effect, that is, to reduce the importance of acetalization products but also the C4/(C6 + C8) product ratio. The incorporation of mesoporosity improves the mobility of intermediate products and increases the C4/(C6 + C8) ratio.

## Supplementary material

As mentioned in the text, some of the data have been included as supplementary material. They include $N_2$ adsorption/desorption isotherms, TPD profiles of adsorbed $CO_2$, illustration of carbonate species formed due to $CO_2$ sorption, mesopore size distributions, XRD patterns, and $^{27}Al$ NMR spectra, as well as comparisons of carbon yields and selectivities.

## Acknowledgement

This research has been funded by Abengoa Research.

## Appendix A. Supplementary data

Supplementary data associated with this article can be found, in the online version, at http://dx.doi.org/10.1016/j.apcata.2014.11.018.

## References

[1] H.-J. Chae, T.-W. Kim, Y.-K. Moon, H.-K. Kim, K.-E. Jeong, C.-U. Kim, S.-Y. Jeong, Appl. Catal. B 150–151 (2013) 596–604.
[2] Butadiene Product Stewardship Guidance Manual, American Chemistry Council Olefins Panel, American Chemistry Council, 2001, Revised 2010.
[3] J.G. Aston, G. Szasz, H.W. Woolley, F.G. Brickwedde, J. Chem. Phys. 14 (1946) 67–79.
[4] F.J. Dumez, G.F. Froment, Ind. Eng. Chem. Process Des. Dev. 15 (1976) 291–301.
[5] M.D. Jones, C.G. Keir, C. Di Iulio, R.A.M. Robertson, C.V. Williams, D.C.I. Apperley, Catal. Sci. Tech. 1 (2011) 267–272.
[6] L.R. Lynd, R.T. Elamder, C.E. Wyman, Appl. Biochem. Biotechnol. 57 (1996) 741–761.
[7] C.E. Wyman, Annu. Rev. Energy Environ. 24 (1999) 189–226.
[8] J.R. Mielenz, Curr. Opin. Microbiol. 4 (2001) 324–329.
[9] C.N. Hamelinck, G.V. Hooijdonk, A.P. Faaij, Biomass Bioenergy 28 (2005) 384–410.
[10] S. Phillips, Ind. Eng. Chem. Res. 46 (2007) 8887–8897.
[11] J.J. Spivey, A. Egbebi, Chem. Soc. Rev. 36 (2007) 1514–1528.
[12] H. van der Heijden, K.J. Ptasinski, Energy 46 (2012) 200–210.
[13] A. Dutta, M. Talmadge, J. Hensley, M. Worley, D. Dudgeon, D. Barton, P. Groenendijk, D. Ferrari, B. Stears, E. Searcy, Environ. Prog. Sustain. Energy 31 (2012) 182–190.
[14] S. Kvisle, A. Aguero, R. Sneeden, Appl. Catal. 43 (1988) 117–131.
[15] S. Bhattacharyya, S. Sanyal, J. Catal. 7 (1967) 152–158.
[16] E. Makshina, W. Janssens, B. Sels, P. Jacobs, Catal. Today 198 (2012) 338–344.
[17] H. Jones, E. Stahly, B. Corson, J. Am. Chem. Soc. 71 (1949) 1822–1828.
[18] M. León, E. Díaz, S. Ordóñez, Catal. Today 164 (2011) 436–442.
[19] W. Ji, Y. Chen, H.H. Kung, Appl. Catal. A 161 (1997) 93–104.
[20] L.M. Baigrie, R.A. Cox, H. Slebocka-Tilk, M. Tencer, T.T. Tidwell, J. Am. Chem. Soc. 107 (1985) 3640–3645.
[21] R.N. Hayes, R.P. Grese, M.L. Gross, J. Am. Chem. Soc. 111 (1989) 8336–8341.
[22] O. Kikhtyanin, V. Kelbichová, D. Vitvarová, M. Kubů, D. Kubička, Catal. Today 227 (2014) 154–162.
[23] E. Dumitriu, V. Hulea, N. Bilba, G. Carja, A. Azzouz, J. Mol. Catal. 79 (1993) 175–185.
[24] A. Biaglow, J. Sepa, R. Gorte, D. White, J. Catal. 151 (1995) 373–384.
[25] E. Dumitriu, A. Azzouz, V. Hulea, D. Lutic, H. Kessler, Microp. Mater. 10 (1997) 1–17.
[26] Y.-C. Chang, A.-N. Ko, Appl. Catal. A 190 (2000) 149–155.
[27] E. Dumitriu, V. Hulea, I. Fechete, A. Auroux, J.-F. Lacaze, C. Guimon, Microp. Mesop. Mater. 43 (2001) 341–359.
[28] S. Luo, J.L. Falconer, Catal. Lett. 57 (1999) 89–93.
[29] B. Noziere, A. Cordova, J. Phys. Chem. A 112 (2008) 2827–2837.

[30] D. Tichit, D. Lutic, B. Coq, R. Durand, R. Teissier, J. Catal. 219 (2003) 167–175.
[31] M. Singh, N. Zhou, D.K. Paul, K. Klabunde, J. Catal. 260 (2008) 371–379.
[32] J.E. Rekoske, M.A. Barteau, Ind. Eng. Chem. Res. 50 (2011) 41–51.
[33] D. Barthomeuf, J. Phys. Chem. 88 (1984) 42–45.
[34] D. Barthomeuf, J. Phys. Chem. 97 (1993) 10092–10096.
[35] D. Barthomeuf, Microp. Mesop. Mater. 66 (2003) 1–14.
[36] D. Vinek, H. Noller, M. Ebel, K. Schwarz, J. Chem. Soc., Faraday Trans. 73 (1977) 734–746.
[37] S.M. Csicsery, Zeolites 4 (1984) 202–213.
[38] A. Corma, J. Catal. 216 (2003) 298–312.
[39] J. Jae, G.A. Tompsett, A.J. Foster, K.D. Hammond, S.M. Auerbach, R.F. Lobo, G.W. Huber, J. Catal. 279 (2011) 257–268.
[40] Y. Lee, S.W. Carr, J.B. Parise, Chem. Mater. 10 (1998) 2561–2570.
[41] T. Frising, P. Leflaive, Microp. Mesop. Mater. 114 (2008) 27–63.
[42] G. Xiong, Y. Yu, Z.-C. Feng, Q. Xin, F.-S. Xiao, C. Li, Microp. Mesop. Mater. 42 (2001) 317–323.
[43] G.H. Kuhl, Zeolites 7 (1987) 451–457.
[44] J. Chang Kim, H.-X. Li, C.-Y. Chen, M. Davis, Microp. Mater. 2 (1994) 413–423.
[45] M.M.J. Treacy, J.B. Higgins, Collection of Simulated XRD Powder Patterns for Zeolites, 5th ed., Elsevier, Amsterdam, The Netherlands, 2007.
[46] J. Turkevich, S. Ciborowski, J. Phys. Chem. 71 (1967) 3208–3217.
[47] E. Lippmaa, A. Samoson, M. Magi, J. Am. Chem. Soc. 108 (1986) 1730–1735.
[48] J. Klinowski, J. Thomas, C. Fyfe, G. Gobbi, J. Hartman, Inorg. Chem. 22 (1983) 63–66.
[49] R. Pierotti, J. Rouquerol, Pure Appl. Chem. 57 (1985) 603–619.
[50] D. Bonenfant, M. Kharoune, P. Niquette, M. Mimeault, R. Hausler, Sci. Technol. Adv. Mater. 9 (2008) 013007.
[51] D. Barthomeuf, Catal. Rev. 38 (1996) 521–612.
[52] J. Di Cosimo, V. Díez, M. Xu, E. Iglesia, C. Apesteguıa, J. Catal. 178 (1998) 499–510.
[53] M.A. Aramendıá, V. Borau, C. Jiménez, J.M. Marinas, J.R. Ruiz, F.J. Urbano, J. Appl. Catal. A 244 (2003) 207–215.
[54] M.A. Aramendía, V. Borau, C. Jiménez, J.M. Marinas, J.R. Ruiz, F.J. Urbano, J. Colloid Interf. Sci. 238 (2001) 385–389.
[55] T. Seki, H. Kabashima, K. Akutsu, H. Tachikawa, H. Hattori, J. Catal. 204 (2001) 393–401.
[56] W.K. Busfield, R.M. Lee, D. Merigold, J. Chem. Soc., Faraday Trans. 69 (1973) 936–940.
[57] M.R. Capeletti, L. Balzano, G. de la Puente, M. Laborde, U. Sedran, Appl. Catal. A 198 (2000) L1–L4.
[58] Y. Zhu, G.-K. Chuah, S. Jaenicke, J. Catal. 241 (2006) 25–33.
[59] Y.-J. Tu, Y.-W. Chen, C. Li, J. Mol. Catal. 89 (1994) 179–189.
[60] K.S. Walton, M.B. Abney, M. Douglas Le Van, Microp. Mesop. Mater. 91 (2006) 78–84.
[61] K.H. Lim, C.P. Grey, J. Am. Chem. Soc. 122 (2000) 9768–9780.
[62] E. Jaramillo, S.M. Auerbach, J. Phys. Chem. B 103 (1999) 9589–9594.
[63] D.H. Olson, Zeolites 15 (1995) 439–443.
[64] D. Murphy, P. Massiani, R. Franck, D. Barthomeuf, J. Phys. Chem. 100 (1996) 6731–6738.
[65] E.A. Pidko, R.A. van Santen, Theoretical chemistry of zeolite reactivity, in: J. Cejka, A. Corma, S. Zones (eds.), Zeolites and Catalysis: Synthesis, Reactions and Applications, Chapter 13, Vol. 1, Wiley-VCH, Weinheim, 2010.
[66] E.A. Pidko, P. Mignon, P. Geerlings, R.A. Schoonheydt, R.A. van Santen, J. Phys. Chem. C 112 (2008) 5510–5519.
[67] Y. Li, R.T. Yang, J. Phys. Chem. B 110 (2006) 17175–17181.
[68] M. Iwama, Y. Suzuki, J. Plévert, K. Itabashi, M. Ogura, T. Okubo, Cryst. Growth Des. 10 (2010) 3471–3479.
[69] S. Caldarelli, A. Buchholz, M. Hunger, J. Am. Chem. Soc. 123 (2001) 7118–7123.
[70] E. Gallei, G. Stumpf, J. Colloid Interf. Sci. 55 (1976) 415–420.
[71] K. Sato, Y. Nishimura, N. Matsubayashi, M. Imamura, H. Shimada, Microp. Mesop. Mater. 59 (2003) 133–146.